Physical Sidelink Control Channel (PSCCH) in Mode 2: Performance Analysis

David W. Griffith, Fernando J. Cintrón, Richard A. Rouil
National Institute of Standards and Technology
Gaithersburg, MD 20899, USA
Email: {david.griffith, fernando.cintron, richard.rouil}@nist.gov

***Abstract*—User Equipments (UEs) that send data must advertise the upcoming transmission by broadcasting signaling messages over the Physical Sidelink Control Channel (PSCCH). Thus, it is important for the network operator to define the PSCCH resource pool to maximize the probability that each UE will be able to successfully decode all of the control messages that appear on the PSCCH. For UEs operating in Mode 2 (i.e., outside the coverage area of an eNodeB), this is especially challenging because there is no base station present that can assign PSCCH resources. UEs must choose pool resources randomly, which can lead to collisions of transmitted messages. In addition, UEs are half-duplex and a poorly designed control channel resource pool can create a significant risk that a signaling message and its duplicate will be missed by a UE that transmits its own signaling message in the same pair of subframes. In this paper, we present an analytical model that allows us to develop closed form expressions for the distribution of the number of UEs that successfully receive a transmitted message on the PSCCH. This model can support PSCCH design by network operators, and can be used to investigate other aspects of D2D communications.**

I. Introduction

The 3rd Generation Partnership Project (3GPP) introduced Proximity Services (ProSe) for Long Term Evolution (LTE) in Release 12 [1]. ProSe enables direct discovery of nearby UEs, and direct communication over a sidelink (rather than the cellular uplink or downlink) without relying on an evolved Node-B (eNB) to do coordination. While direct discovery is envisioned for the general public, direct communication is enabled for public safety users only.

Public safety users require Device-to-Device (D2D) communications when cellular coverage is not available, i.e., out-of-coverage. Out-of-coverage scenarios include remote areas lacking network infrastructure, inside buildings with deep fades, and during service outages. ProSe allows network operators to configure UEs to operate out-of-coverage, which is defined as Mode 2 [2]. Unfortunately, the lack of coordination between devices can degrade the communication performance.

In Mode 2, UEs must contend for resources in all sidelink channels. This paper develops a model of contention effects in the Physical Sidelink Control Channel (PSCCH), which carries signaling traffic that is vital for D2D data communications. We provide an overview of D2D communications in Section II, and derive the distribution of the number of UEs that receive a message over the PSCCH in Section III. In Section IV, we validate the model and discuss the network operator guidelines for PSCCH design that the model provides. We summarize our results in Section V.

II. Device-to-Device Communication

A. Overview and Prior Work

Communication over the sidelink uses communication periods that are periodic in the time domain. Each sidelink period includes instances of the PSCCH and the Physical Sidelink Shared Channel (PSSCH), which carries data. 3GPP defines procedures related to the transmission and reception on the PSCCH and PSSCH in [3, Clause 14]. All UEs are preconfigured by the network operator with the period duration, PSCCH configuration, and PSSCH configuration so that they can operate autonomously when out-of-coverage. Instead of using PSCCH resources that are assigned by an eNB, UEs with data to send select random resources from the PSCCH resource pool to send a control message that tells potential receivers, all of which monitor the PSCCH, where and how the transmitting UE's pending data will be transmitted in the PSSCH. Upon successful reception of a control message, a UE can tune to the indicated Physical Resource Blocks (PRBs) in the PSSCH. Any UEs that fail to receive and decode the PSCCH message will not be able to receive the advertised data transmission in the PSSCH.

A general description of the PSCCH and other D2D control channels is available from Lien et al. in [4] and [5]. A more detailed analysis by Shih et al. in [6] describes the PSCCH and PSSCH and derives a simple expression for PSCCH transmission success. The formula matches Eq. (20) in this paper, but does not include the half-duplex effect.

B. Physical Sidelink Control Channel

All control messages in a given period are sent twice; an initial transmission that occupies one PRB is followed by a duplicate transmission in a second PRB in the same period. UEs randomly select PRB pairs from the PSCCH resource pool, which is defined by the following pair of parameters: L_{PSCCH}, the number of subframes that the pool spans in the time domain ($2 \leq L_{PSCCH} \leq 40$), and $M_{RB}^{PSCCH\_RP}$, the number of PRBs that the pool spans in the frequency domain

[3, Clause 14.2.3]. Because each message transmission uses two PRBs, the number of available resources in the pool is $N_{PSCCH} = L_{PSCCH} \times \lfloor M_{RB}^{PSCCH\_RP}/2 \rfloor$.

III. Analytical Model

In this section, we develop the mathematical model that describes the ability of UEs in a D2D group containing N_u UEs to receive messages on the PSCCH. Each UE broadcasts a message over the PSCCH to all other UEs in the group. Let $\mathcal{R}_n^C$ be the event, "n UEs out of $(N_u - 1)$ UEs receive a message from a random UE in the group," where $0 \le n \le N_u - 1$. Note that when $\mathcal{R}_n^C$ occurs, at most n UEs will receive the data that the transmitting UE will send on the PSSCH. We will derive the distribution of $\mathcal{R}_n^C$ in this section.

A. Operation of the PSCCH

UEs with data to send randomly pick a resource from the pool and use the pair of PRBs associated with that resource to send a transmission advertisement. The resource index n_{PSCCH} is thus a discrete uniform random variable, $0 \le n_{PSCCH} < N_{PSCCH}$, and the mapping from n_{PSCCH} to the PRB pair occupying subframe ℓ_{b1} and PRB m_{a1}, and subframe ℓ_{b2} and PRB m_{a2}, where $0 \le a1, a2 < L_{PSCCH}$ and $0 \le b1, b2 < M_{RB}^{PSCCH\_RP}$ is (see [3, Clause 14.2.1.1])

$$a1 = \lfloor n_{PSCCH}/L_{PSCCH} \rfloor \tag{1a}$$

$$b1 = n_{PSCCH} \bmod L_{PSCCH} \tag{1b}$$

and

$$a2 = \left\lfloor \frac{n_{PSCCH}}{L_{PSCCH}} \right\rfloor + \left\lfloor \frac{M_{RB}^{PSCCH\_RP}}{2} \right\rfloor \tag{2a}$$

$$b2 = \left(n_{PSCCH} + 1 + \left\lfloor \frac{n_{PSCCH}}{L_{PSCCH}} \right\rfloor \bmod (L_{PSCCH} - 1) \right) \bmod L_{PSCCH}. \tag{2b}$$

We show an example of the resource mapping in Eqs. (1) and (2) in Fig. 1. As the figure shows, Eq. (1) fills the lower half of the pool, starting with 0 in the lower left hand corner and filling the pool by proceeding from left to right and from the bottom row to the top row of the lower half. Eq. (2) fills the upper half of the pool by starting in the next-to-leftmost subframe in the bottom row of the upper half, and filling from left to right, then wrapping around to the left of the current row before proceeding to the next higher row. The starting subframe in row $a2$ is one to the right from the starting subframe in row $(a2 - 1)$, and increasing resource indexes wrap around to the left, as shown in the figure.

We define $L \stackrel{\text{def}}{=} L_{PSCCH}$, $M \stackrel{\text{def}}{=} M_{RB}^{PSCCH\_RP}$, and $N \stackrel{\text{def}}{=} N_{PSCCH}$ in order to make the mathematical expressions in the following more compact. We assume that all UEs are half-duplex; i.e., two UEs that transmit in the same subframe will not receive each other's messages that were sent during that subframe.

Since a UE successfully decodes a PSCCH message if it can receive at least one transmission, we need to determine which resource selections by a UE will prevent it from receiving another UE's transmission. We begin by examining an arbitrary pair of UEs in the D2D group that we call the receiving UE and the transmitting UE. These two UEs independently choose resources. One of the following events will occur:

- $\mathcal{X}$ (Collision): The transmitting and receiving UEs choose the same resource.
- $\mathcal{O}_2$ (Two column overlap): The transmitting and receiving UEs choose resources such that each of their respective PRBs lie in the same subframe (note that $\mathcal{X} \subseteq \mathcal{O}_2$).
- $\mathcal{O}_1$ (One column overlap): The transmitting and receiving UEs choose different resources, such that one of the transmitter's PRBs is in the same subframe as one of the receiver's PRBs, while the UEs' other PRBs lie in different subframes.
- $\mathcal{O}_0$ (Zero column overlap): The transmitting and receiving UEs choose different resources, such that neither UE's PRBs overlaps the other UE's PRBs.

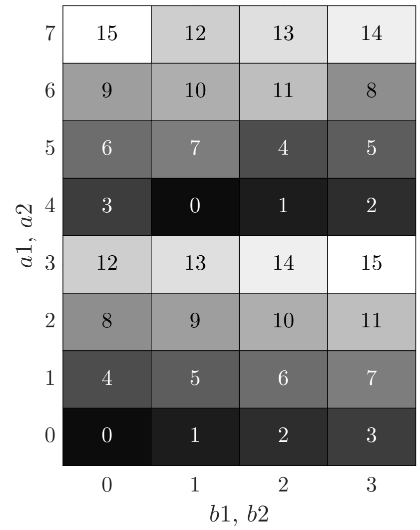

Fig. 1: Example PSCCH pool with $L_{PSCCH} = 4$ subframes and $M_{RB}^{PSCCH\_RP} = 8$ PRBs, with n_{PSCCH} values shown in each PRB.

In Fig. 2, we show examples of the each of the events described above. In each case shown in the figure, the transmitting UE has chosen $n_{PSCCH} = 0$. We show the Venn diagram associated with events $\mathcal{O}_0$, $\mathcal{O}_1$, and $\mathcal{O}_2$ in Fig. 3. We observe that the events are non-intersecting, and that the collision event $\mathcal{X}$ is a special case of event $\mathcal{O}_2$. This allows us to partition $\mathcal{O}_2$ into events $\mathcal{O}_2 \cap \mathcal{X}$ and $\mathcal{O}_2 \cap \overline{\mathcal{X}}$, where $\overline{\mathcal{X}}$ is the complement of event $\mathcal{X}$.

If two UEs' transmissions overlap in both of their chosen subframes, then event $\mathcal{X} \subseteq \mathcal{O}_2$ occurs if the two UEs pick the same resource, which results in a collision. Also, we assume that a collision blocks the transmitter UE's message for all UEs in the group[1]. Event $\mathcal{O}_2 \cap \mathcal{X}$ occurs if the

[1] In practice, one colliding message may still be received if the signal-to-interference ratio (SIR) is high enough. We assume that this does not occur, which simplifies the analysis and gives us a more conservative model. Our ongoing work will consider the effect of SIR.

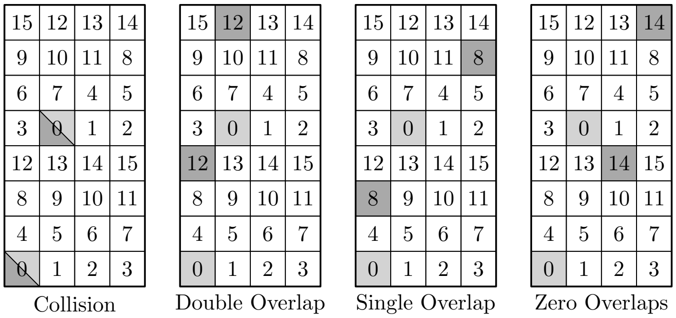

Fig. 2: Examples of UE interaction events $\mathcal{X}$, $\mathcal{O}_0$, $\mathcal{O}_1$, and $\mathcal{O}_2$.

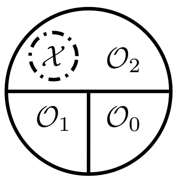

Fig. 3: Venn diagram for interactions between the resource selections by two UEs (dashed lines indicate that $\mathcal{X} \subseteq \mathcal{O}_2$).

receiver picks a resource that is different from the transmitter's resource, but which maps to a pair of PRBs that lie in the same two subframes as the PRB pair used by the transmitter. The half-duplex effect prevents the receiver from receiving either copy of the transmitter's message. If events $\mathcal{O}_0$ or $\mathcal{O}_1$ occur, a receiver will be able to receive at least one copy of the transmitter's message, assuming no other UEs pick the transmitter's chosen resource and cause a collision.

We condition on whether at least one of the $(N_u - 1)$ UEs picks the transmitter's resource index and causes a collision. We define $\mathcal{C}$ to be the event, "a collision occurred between the transmitter and at least one other UE." The complement $\overline{\mathcal{C}}$ is be the event that no collisions occurred between the transmitter and any other UE. We have

$$\begin{aligned}\mathsf{Pr}\{\mathcal{R}_n^C\} &= \mathsf{Pr}\{\mathcal{R}_n^C \,|\, \mathcal{C}\}\mathsf{Pr}\{\mathcal{C}\} + \mathsf{Pr}\{\mathcal{R}_n^C \,|\, \overline{\mathcal{C}}\}\mathsf{Pr}\{\overline{\mathcal{C}}\} \\ &= \left[1 - \left(1 - \tfrac{1}{N}\right)^{N_u - 1}\right]\delta[n] \\ &\quad + \left(1 - \tfrac{1}{N}\right)^{N_u - 1} \mathsf{Pr}\{\mathcal{R}_n^C \,|\, \overline{\mathcal{C}}\}, \end{aligned} \tag{3}$$

where $\delta[n]$ is the (discrete) Kronecker delta function:

$$\delta[n] = \begin{cases} 1, & n = 0 \\ 0, & n \neq 0 \end{cases}.$$

To obtain Eq. (3), we observe that $\mathsf{Pr}\{\overline{\mathcal{C}}\} = \left(1 - \frac{1}{N}\right)^{N_u - 1}$ because the UEs pick resources independently, and a single receiving UE picks the transmitter's resource with probability $1/N$. Thus $\mathsf{Pr}\{\overline{\mathcal{C}}\}$ is the probability that none of the $(N_u - 1)$ receiving UEs pick the transmitter's resource. Next, $\mathsf{Pr}\{\mathcal{R}_n^C \,|\, \mathcal{C}\} = 0$ when $n > 0$, since a collision prevents any UE from receiving either copy of the transmitting UE's message. Thus for $n = 0$, $\mathsf{Pr}\{\mathcal{R}_0^C \,|\, \mathcal{C}\} = 1$, and $\mathsf{Pr}\{\mathcal{R}_n^C\}$ contains an additive term that is present only when $n = 0$. Finally, $\mathsf{Pr}\{\mathcal{R}_n^C \,|\, \overline{\mathcal{C}}\} \neq 0$ when $n = 0$, since it is possible for all the other UEs to pick resources that are different from the one picked by the transmitting UE, but that their resources can map to PRBs that lie in the same pair of subframes as those used by the transmitting UE.

B. Computing $\mathsf{Pr}\{\mathcal{R}_n^C \,|\, \overline{\mathcal{C}}\}$

In order to get $\mathsf{Pr}\{\mathcal{R}_n^C \,|\, \overline{\mathcal{C}}\}$, we can treat the resource selection process as a set of independent trials, each of which results in one of two possible outcomes. A trial succeeds if events $\mathcal{O}_0$ or $\mathcal{O}_1$ occur; it fails if event $\mathcal{O}_2$ occurs. From the form of Eq. (3), the success and failure probabilities for each receiving UE are conditioned on no collision with the transmitting UE, and are $\mathsf{Pr}\{\mathcal{O}_0 \cup \mathcal{O}_1 \,|\, \overline{\mathcal{X}}\}$ and $\mathsf{Pr}\{\mathcal{O}_2 \,|\, \overline{\mathcal{X}}\}$, respectively. From the Venn diagram in Fig. 3, the conditional success probability is

$$\mathsf{Pr}\{\mathcal{O}_0 \cup \mathcal{O}_1 \,|\, \overline{\mathcal{X}}\} = \frac{\mathsf{Pr}\{\mathcal{O}_0 \cup \mathcal{O}_1\}}{\mathsf{Pr}\{\overline{\mathcal{X}}\}} = \frac{\mathsf{Pr}\{\mathcal{O}_0\} + \mathsf{Pr}\{\mathcal{O}_1\}}{\mathsf{Pr}\{\overline{\mathcal{X}}\}}, \tag{4}$$

since $\mathcal{O}_0 \cup \mathcal{O}_1 \subseteq \overline{\mathcal{X}}$, and $\mathcal{O}_0 \cap \mathcal{O}_1 = \varnothing$. Similarly, the conditional failure probability is

$$\mathsf{Pr}\{\mathcal{O}_2 \,|\, \overline{\mathcal{X}}\} = \mathsf{Pr}\{\mathcal{O}_2 \cap \overline{\mathcal{X}}\}/\mathsf{Pr}\{\overline{\mathcal{X}}\}. \tag{5}$$

Since $\mathsf{Pr}\{\mathcal{R}_n^C \,|\, \overline{\mathcal{C}}\}$ follows a binomial distribution, we use the success probability from Eq. (4) and the failure probability from Eq. (5) and get

$$\begin{aligned}&\mathsf{Pr}\{\mathcal{R}_n^C \,|\, \overline{\mathcal{C}}\} \\ &\quad = \binom{N_u - 1}{n} \frac{\left(\mathsf{Pr}\{\mathcal{O}_0 \cup \mathcal{O}_1\}\right)^n \left(\mathsf{Pr}\{\mathcal{O}_2 \cap \overline{\mathcal{X}}\}\right)^{N_u - n - 1}}{\left(1 - \frac{1}{N}\right)^{N_u - 1}}. \end{aligned} \tag{6}$$

Inserting Eq. (6) into Eq. (3) and canceling the common term $\left(1 - \frac{1}{N}\right)^{N_u - 1}$ gives

$$\begin{aligned}&\mathsf{Pr}\{\mathcal{R}_n^C\} \\ &\quad = \left[1 - \left(1 - \tfrac{1}{N}\right)^{N_u - 1}\right]\delta[n] \\ &\qquad + \binom{N_u - 1}{n} \left(\mathsf{Pr}\{\mathcal{O}_0 \cup \mathcal{O}_1\}\right)^n \left(\mathsf{Pr}\{\mathcal{O}_2 \cap \overline{\mathcal{X}}\}\right)^{N_u - n - 1}. \end{aligned} \tag{7}$$

We evaluate Eq. (7) by considering the structure of the resource pool. As shown in Fig. 4 for the case where $L_{PSCCH} = 4$ subframes and $M_{RB}^{PSCCH\_RP} = 8$ PRBs, one can show using Eqs. (1) and (2) that in general the PSCCH resource mapping is rotationally invariant. In other words, for all PRBs with a given PRB index m_{a1}, the position of the PRB (ℓ_{b2}, m_{a2}) relative to the PRB (ℓ_{b1}, m_{a1}) is the same, modulo $L_{PSCCH} - 1$. The fortuitous effect of this property is that we do not have to condition on which subframe is occupied by the transmitter's first transmission.

From Figs. 1 and 4, for each subframe, the copies of the resources in the lower (upper) half of the subframe are arranged in the same repeating pattern in the upper (lower) half of the subframe, as shown in Fig. 5. By partitioning the first subframe into two $(M/2) \times 1$ vectors, which are shaded differently in Fig. 4, we can see that the copies of the elements of the lower vector appear as diagonals that occupy the upper

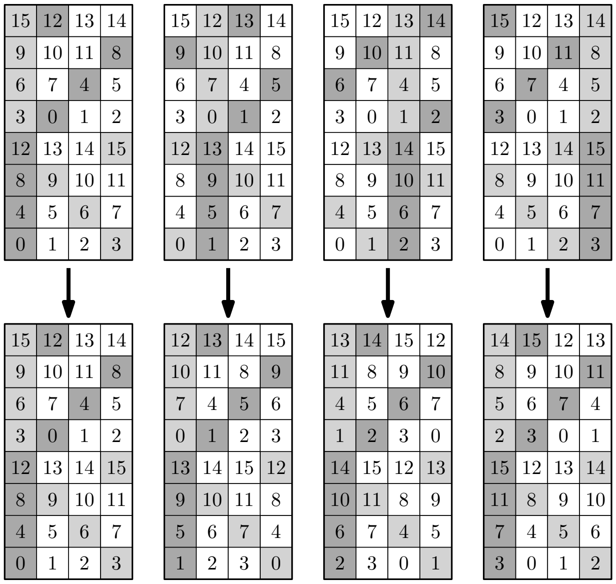

Fig. 4: Example of rotational invariance in the PSCCH, for $L_{PSCCH} = 4$ subframes and $M_{RB}^{PSCCH\_RP} = 8$ PRBs.

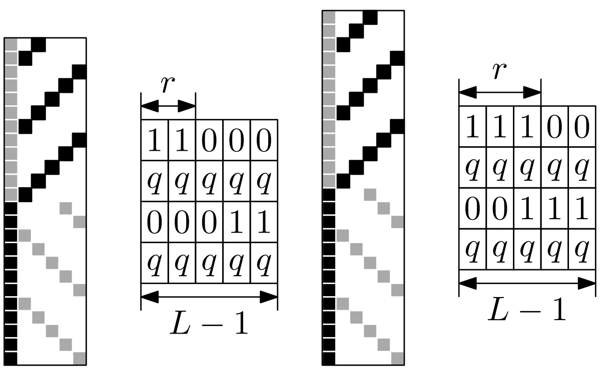

(a) Case 1: $0 \leq r \leq \left\lfloor \frac{L-1}{2} \right\rfloor$ (b) Case 2: $\left\lfloor \frac{L-1}{2} \right\rfloor < r \leq L-2$

Fig. 5: Plots of example PSCCH pools that illustrate the two cases determined by the value of r.

rows of the pool and that the elements of the lower vector, if read from bottom to top, fill the diagonals in an ascending fashion, going from left to right. Likewise, the elements of the upper vector fill diagonals in an ascending fashion from right to left in the lower half of the pool.

We can map the diagonal patterns to a $4 \times (L-1)$ occupancy grid, shown in Fig. 5. Let "Subframe 0" be the leftmost subframe. We define the following two quantities:

$$q \stackrel{\text{def}}{=} \lfloor (M/2)/(L-1) \rfloor \tag{8}$$

$$r \stackrel{\text{def}}{=} \frac{M}{2} \bmod (L-1), \tag{9}$$

so that

$$\frac{M}{2} = (L-1)q + r. \tag{10}$$

From Fig. 5, the second copies of the elements of each length-$(M/2)$ subvector in Subframe 0 form q complete diagonals with r elements forming a partial final diagonal. The final diagonal in the upper part of the PSCCH starts in Subframe 1 and extends rightward, while the final diagonal in the lower part of the PSCCH starts in Subframe $(L-1)$ and extends leftward.

There are two cases to consider, which depend on the value of r. Case 1 occurs when $0 \leq r \leq \lfloor (L-1)/2 \rfloor$; in this case, the partial diagonals do not overlap, as shown in Fig. 5a. Note that when $r = 0$ we have a set of q complete diagonals that appear over Subframes 1 through $(L-1)$, with no partial diagonal present. Case 2 occurs when $\lfloor (L-1)/2 \rfloor < r < L-1$; here, the partial diagonals overlap, as shown in Fig. 5b.

From Fig. 5a, for Case 1, $2r$ subframes contain $(2q+1)$ messages that are duplicates of messages in Subframe 0; the remaining $(L-2r-1)$ subframes each contain $2q$ duplicate messages from Subframe 0. For Case 2, there are $2(L-r-1)$ subframes containing $(2q+1)$ duplicate messages from Subframe 0, and the remaining $(2r-L+1)$ subframes each contain $(2q+2)$ duplicate messages from Subframe 0. We will use these facts in the following to obtain the conditional success and failure probabilities that compose Eq. (7).

C. Deriving $\Pr\{\mathcal{O}_0\}$

Let n_τ and n_ρ be the resource indexes respectively chosen by the transmitting and receiving UEs. We rotate the PSCCH grid so that one of the transmitting UE's two PRBs is in the first column (subframe s_0). Next, we label the subframes in the pool from left to right as follows: $s_0, s_1, \ldots, s_{L-1}$, so that one of the transmitter's PRBs lies in s_0, i.e., $\{n_\tau \in s_0\}$. Let s_τ be the subframe where the second PRB associated with n_τ occurs. By definition, $\mathcal{O}_0 = \{n_\rho \notin s_0\} \cap \{n_\rho \notin s_\tau\}$. We condition on the subframe occupied by the second PRB associated with n_τ, and get

$$\Pr\{\mathcal{O}_0\} = \sum_{i=1}^{L-1} \Pr\{\mathcal{O}_0 \,|\, n_\tau \in s_i\} \Pr\{n_\tau \in s_i\}. \tag{11}$$

To evaluate Eq. (11), we examine $\Pr\{n_\tau \in s_i\}$. For Case 1, there are $2r$ subframes where $\Pr\{n_\tau \in s_i\} = (2q+1)/M$ and $(L-2r-1)$ subframes where $\Pr\{n_\tau \in s_i\} = (2q)/M$. For Case 2, there are $2(L-r-1)$ subframes where $\Pr\{n_\tau \in s_i\} = (2q+1)/M$ and $(2r-L+1)$ subframes where $\Pr\{n_\tau \in s_i\} = (2q+2)/M$.

Next, we consider $\Pr\{\mathcal{O}_0 \,|\, n_\tau \in s_i\}$. Fig. 6 shows an example where $n_\tau \in s_1$. Since there are no subframe overlaps, and $n_\tau \in s_0$, then $n_\rho \notin s_0$. In Fig. 6, $n_\tau \in \{0, 9, 12\}$; if the receiver chooses one of the other resources whose PRBs s_1, which are shaded light blue in Fig. 6, $\mathcal{O}_0$ cannot occur. The only choices that result in no overlaps are $n_\rho \in \{2, 11, 14\}$, The number of resources that the receiver can pick is N_{PSCCH} minus the number of resources in s_0 (M), minus the number of resources in s_1 that are not in s_0 (5 resources in the example). Thus $\Pr\{\mathcal{O}_0 \,|\, n_\tau \in s_1\} = (16-8-5)/16 = 3/16$.

In general, for Case 1, there are $2r$ subframes where $\Pr\{\mathcal{O}_0 \,|\, n_\tau \in s_i\} = (N-2M+2q+1)/N$ and $(L-2r-1)$ subframes where $\Pr\{\mathcal{O}_0 \,|\, n_\tau \in s_i\} = (N-2M+2q)/N$. For Case 2, there are $2(L-r-1)$ subframes where $\Pr\{\mathcal{O}_0 \,|\, n_\tau \in s_i\} = (N-2M+2q+1)/N$ and $(2r-L+1)$ subframes where $\Pr\{\mathcal{O}_0 \,|\, n_\tau \in s_i\} = (N-2M+2q+2)/N$.

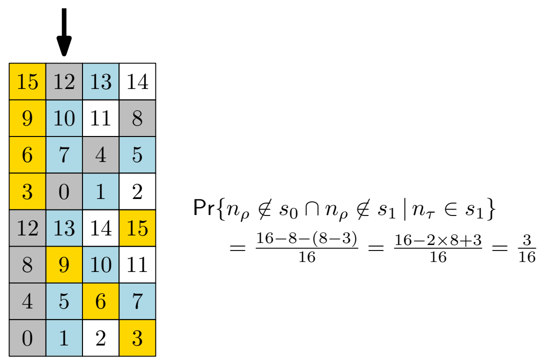

Fig. 6: Example of possible double subframe overlaps when $n_\tau \in s_1$, for $L_{PSCCH} = 4$ subframes and $M_{RB}^{PSCCH\_RP} = 8$ PRBs.

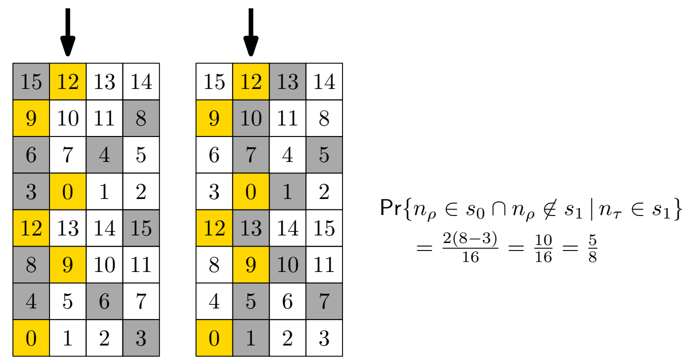

Fig. 7: Example of possible single subframe overlaps when $n_\tau \in s_1$, for $L_{PSCCH} = 4$ subframes and $M_{RB}^{PSCCH\_RP} = 8$ PRBs.

We now evaluate Eq. (11). We can simplify our result by replacing N with $LM/2$ and using Eq. (10). For Case 1,

$$\begin{aligned}\mathrm{Pr}\{\mathcal{O}_0\} &= (2r)\frac{(N-2M+2q+1)(2q+1)}{MN} \\ &\quad + (L-2r-1)\frac{(N-2M+2q)(2q)}{MN} \\ &= \frac{(L-4)M^2+4qM+4(2q+1)r}{LM^2}, \end{aligned} \tag{12}$$

and for Case 2,

$$\begin{aligned}\mathrm{Pr}\{\mathcal{O}_0\} &= 2(L-r-1)\frac{(N-2M+2q+1)(2q+1)}{MN} \\ &\quad + (2r-L+1)\frac{(N-2M+2q+2)(2q+2)}{MN} \\ &= \frac{(L-4)M^2+4qM+4(2q+3)r-4(L-1)}{LM^2}. \end{aligned} \tag{13}$$

D. *Deriving* Pr{$\mathcal{O}_1$}

Next, we consider a single subframe overlap. If we rotate the PSCCH so that $n_\rho \in s_0$, the event $\mathcal{O}_1$ occurs when $n_\rho \notin s_\tau$. Conditioning on the second subframe occupied by n_τ, we get

$$\mathrm{Pr}\{\mathcal{O}_1\} = \sum_{i=1}^{L-1} \mathrm{Pr}\{\mathcal{O}_1 \,|\, n_\tau \in s_i\}\,\mathrm{Pr}\{n_\tau \in s_i\}. \tag{14}$$

We obtained expressions for Pr{$n_\tau \in s_i$} in our treatment of Pr{$\mathcal{O}_0$}. To get Pr{$\mathcal{O}_1 \,|\, n_\tau \in s_i$}, we examine the example shown in Fig. 7. If $n_\rho \in s_0$ and $n_\tau \in s_1$ (i.e., if $n_\tau \in \{0, 9, 12\}$, which are shaded gold in the figure), then there are two possibilities: $n_\rho \in \{3, 4, 6, 8, 15\}$, or $n_\rho \in \{1, 5, 7, 10, 13\}$. Both sets of resources are shaded gray in the figure. The number of resources that the receiver can pick to get a single overlap is the number of gray resources in both grids, which is $M_{RB}^{PSCCH\_RP}$ minus the number of resources from s_0 that are in s_1. Thus the probability that the receiver picks a resource that results in event $\mathcal{O}_1$ is $2(8-3)/16 = 10/16$.

Generalizing this example, for Case 1, there are $2r$ subframes where Pr{$\mathcal{O}_1 \,|\, n_\tau \in s_i$} $= (M-2q-1)/N$ and there are $(L-2r-1)$ subframes where Pr{$\mathcal{O}_1 \,|\, n_\tau \in s_i$} $= (M-2q)/N$. For Case 2, there are $2(L-r-1)$ subframes where Pr{$\mathcal{O}_1 \,|\, n_\tau \in s_i$} $= (M-2q-1)/N$ and $(2r-L+1)$ subframes where Pr{$\mathcal{O}_1 \,|\, n_\tau \in s_i$} $= (M-2q-2)/N$.

Next we get the expressions for Pr{$\mathcal{O}_1$}. For Case 1,

$$\begin{aligned}\mathrm{Pr}\{\mathcal{O}_1\} &= (2r)\frac{2(M-(2q+1))(2q+1)}{MN} \\ &\quad + (L-2r-1)\frac{2(M-2q)(2q)}{MN} \\ &= \frac{4M^2-8qM-8(2q+1)r}{LM^2}, \end{aligned} \tag{15}$$

and for Case 2,

$$\begin{aligned}\mathrm{Pr}\{\mathcal{O}_1\} &= 2(L-r-1)\frac{2(M-2q-1)(2q+1)}{MN} \\ &\quad + (2r-L+1)\frac{2(M-2q-2)(2q+2)}{MN} \\ &= \frac{4M^2-8qM-8(2q+3)r+8(L-1)}{LM^2}. \end{aligned} \tag{16}$$

E. *Deriving* Pr{$\mathcal{O}_2 \cap \overline{\mathcal{X}}$}

Finally, we examine the case of double overlaps with no collision. Event $\{\mathcal{O}_2 \cap \overline{\mathcal{X}}\}$ occurs when $n_\rho \in s_0$ and $n_\rho \in s_\tau$, but $n_\rho \neq n_\tau$. By conditioning on s_τ, we get

$$\mathrm{Pr}\{\mathcal{O}_2 \cap \overline{\mathcal{X}}\} = \sum_{i=1}^{L-1} \mathrm{Pr}\{\mathcal{O}_2 \cap \overline{\mathcal{X}} \,|\, n_\tau \in s_i\}\mathrm{Pr}\{n_\tau \in s_i\}. \tag{17}$$

In the example shown in Fig. 8, $s_\tau = s_1$, so $n_\tau \in \{0, 9, 12\}$, which are shaded gold in the figure. There are three possibilities. If $n_\tau = 0$, $n_\rho \in \{9, 12\}$, if $n_\tau = 9$, $n_\rho \in \{0, 12\}$, and if $n_\tau = 12$, $n_\rho \in \{0, 9\}$. Note that Pr{$n_\tau = 0 \,|\, n_\tau \in s_1$} $=$ Pr{$n_\tau = 9 \,|\, n_\tau \in s_1$} $=$ Pr{$n_\tau = 12 \,|\, n_\tau \in s_1$} $= 1/3$. As shown in the figure, this means that the conditional probability that $\mathcal{O}_2 \cap \overline{\mathcal{X}}$ holds is $3 \times (1/3) \times (2/16) = 1/8$.

Generalizing this result, for Case 1, we have

- $2r$ subframes where Pr{$\mathcal{O}_2 \cap \overline{\mathcal{X}} \,|\, n_\tau \in s_i$} $= (2q)/N$
- $(L-2r-1)$ subframes where Pr{$\mathcal{O}_2 \cap \overline{\mathcal{X}} \,|\, n_\tau \in s_i$} $= (2q-1)/N$

For Case 2, we have

- $2(L-r-1)$ subframes where Pr{$\mathcal{O}_2 \cap \overline{\mathcal{X}} \,|\, n_\tau \in s_i$} $= (2q)/N$

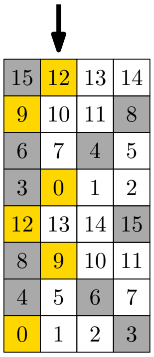

$$\mathsf{Pr}\{\{n_\rho \in s_0\} \cap \{n_\rho \in s_1\} \cap \{n_\rho \neq n_\tau\} \,|\, n_\tau \in s_1\} = \left(\tfrac{1}{3} \times \tfrac{2}{16}\right) + \left(\tfrac{1}{3} \times \tfrac{2}{16}\right) + \left(\tfrac{1}{3} \times \tfrac{2}{16}\right) = \tfrac{1}{8}$$

Fig. 8: Example of double subframe overlap when $n_\tau \in s_1$, for $L_{PSCCH} = 4$ subframes and $M_{RB}^{PSCCH\_RP} = 8$ PRBs.

- $(2r - L + 1)$ subframes where $\mathsf{Pr}\{\mathcal{O}_2 \cap \overline{\mathcal{X}} \,|\, n_\tau \in s_i\} = (2q+1)/N$

Thus for Case 1, we get

$$\begin{aligned}\mathsf{Pr}\{\mathcal{O}_2 \cap \overline{\mathcal{X}}\} &= (2r)\frac{(2q)(2q+1)}{MN} \\ &\quad + (L - 2r - 1)\frac{(2q-1)(2q)}{MN} \\ &= \frac{(4q-2)M + 4(2q+1)r}{LM^2}, \end{aligned} \tag{18}$$

and for Case 2, we get

$$\begin{aligned}\mathsf{Pr}\{\mathcal{O}_2 \cap \overline{\mathcal{X}}\} &= 2(L - r - 1)\frac{(2q)(2q+1)}{MN} \\ &\quad + (2r - L + 1)\frac{(2q+1)(2q+2)}{MN} \\ &= \frac{(4q-2)M + 4(2q+3)r - 4(L-1)}{LM^2}. \end{aligned} \tag{19}$$

We evaluate Eq. (7) by adding Eq. (12) to Eq. (15) (Case 1) or by adding Eq. (13) to Eq. (16) (Case 2) to get $\mathsf{Pr}\{\mathcal{O}_0 \cup \mathcal{O}_1\}$, and by using $\mathsf{Pr}\{\mathcal{O}_2 \cap \overline{\mathcal{X}}\}$ from Eq. (18) (Case 1) or Eq. (19) (Case 2).

IV. Numerical Results and Evaluation

A. Validation

We used two independent methods to validate the analytical model: Monte Carlo experiments performed in Matlab, and network simulations performed using ns-3 [7]. We used a PSCCH pool configuration of 8 subframes by 44 PRBs, and a group size of 6 UEs. Our Monte Carlo experiments consisted of 100 experimental runs with 100 000 trials per run. The network simulations used the same transmission handling assumptions as the theoretical model: half duplex UEs and forced transmission drops resulting from collisions. Each data point used 50 simulation runs, each of which covered 8000 s of activity and used a sidelink communication period of 80 ms, so that we examined 100 000 periods per run.

In both the Matlab Monte Carlo runs and the ns-3 simulations, we randomly assigned resources to each UE, and then determined how many UEs each UE's message could reach, taking collisions and the half duplex effect into account. Once the full set of runs was complete, we obtained two sets

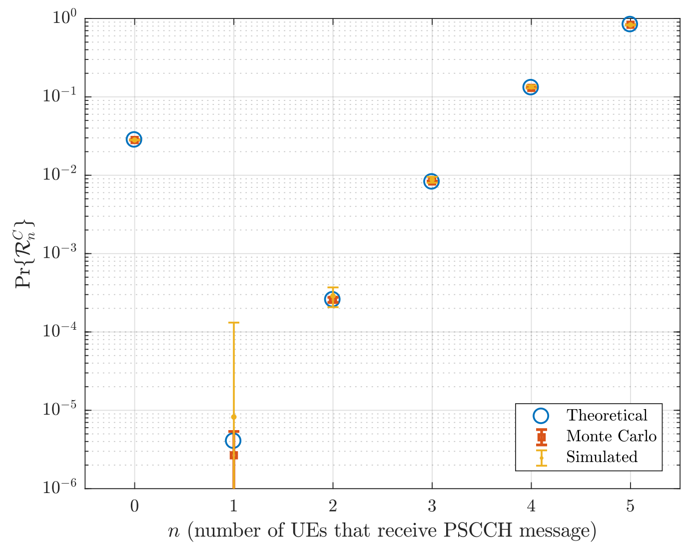

Fig. 9: Validation with 95 % confidence intervals; $N_u = 6$ UEs, $L_{PSCCH} = 8$ subframes, and $M_{RB}^{PSCCH\_RP} = 44$ PRBs.

of estimates of $\mathsf{Pr}\{\mathcal{R}_n^C\}$, one for the ns-3 simulations and one for the Monte Carlo simulations, by dividing $\mathcal{N}_n$, the number of times a UE's transmitted control message reached n other UEs, by the product $N_u \times \mathcal{N}_{\text{periods}}$. This results in one estimate per run. From each set of estimates, we computed estimates of both the mean $\widehat{\mu}_n$ and the standard deviation $\widehat{\sigma}_n$ for $0 \le n \le N_u - 1$; we plot $\widehat{\mu}_n$ in Fig. 9, and we used the estimated standard deviation to produce our 95 % confidence intervals that have the form $[\widehat{\mu}_n - 1.96\widehat{\sigma}_n, \widehat{\mu}_n + 1.96\widehat{\sigma}_n]$.

We present the theoretical results along with the outputs from both validation methods in Fig. 9, with 95 % confidence intervals shown for each simulation result. We note the large confidence interval at $n = 1$ for the results from ns-3 relative to the Monte Carlo results. This is because we used half as many runs in the ns-3 simulations due to time constraints. Moreover, $\mathcal{R}_1^C$ occurs only when $(N_u - 2)$ UEs do not collide with the transmitter but choose resources do that all experience double subframe overlaps, which is very unlikely, and which requires a large number of runs to produce any experimental occurrences of this event. We emphasize that for all values of n, the figure shows very close agreement between the model and the results obtained from both simulations. We obtained similar agreement using other pool configurations and other values of N_u; we do not present these results here due to space limitations.

B. PSCCH Pool Design

Finally, we show how that model can be used to produce design guidelines for network operators. Double overlaps are undesirable because they prevent UEs from receiving control messages, even in the absence of a collision. However, for a pool configured such that $L - 1 \ge M$, Case 1 as defined in Section III-B holds (i.e., $0 \le r \le \lfloor (L-1)/2 \rfloor$), and $q = 0$ and $r = M$. Evaluating Eq. (18) with $q = 0$ and $r = M$

gives $\Pr\{\mathcal{O}_2 \cap \overline{\mathcal{X}}\} = 0$. Evaluating Eq. (12) and Eq. (15) and summing the results gives $\Pr\{\mathcal{O}_0 \cup \mathcal{O}_1\} = 1 - (1/N)$, so that

$$\Pr\{\mathcal{R}_n^C\} = \begin{cases} 1 - \left(1 - \frac{1}{N}\right)^{N_u - 1}, & n = 0 \\ \left(1 - \frac{1}{N}\right)^{N_u - 1}, & n = N_u - 1 \\ 0, & \text{else} \end{cases} \tag{20}$$

Eq. (20) implies that there are two possible outcomes for a pool constructed to avoid double overlaps: a collision occurs that prevents a message from being received by any other UEs, or there is no collision and all UEs receive the transmitted message.

Fig. 10 shows the maximum D2D group size that is possible when $\Pr\{\mathcal{R}_{N_u-1}^C\} \geq 95$ % for various values of L_{PSCCH} and $M_{RB}^{PSCCH\_RP}$. The set of white discs follow the line $M_{RB}^{PSCCH\_RP} = L_{PSCCH} - 1$, and the regions of the figure that are shaded black indicate that it is not possible to support any UEs with the desired level of reliability. While the figure shows that increasing N_{PSCCH} increases the number of UEs that can be supported, it also shows that, for a given value of L_{PSCCH}, the maximum supportable group size is reached when $M_{RB}^{PSCCH\_RP} = L_{PSCCH} - 1$, and that increasing $M_{RB}^{PSCCH\_RP}$ does not produce further increases in the number of supportable UEs. In fact, in many cases the figure shows that further increasing $M_{RB}^{PSCCH\_RP}$ beyond L_{PSCCH} results in reductions in the maximum supportable group size. This is because expanding the pool in the frequency domain reduces $\Pr\{\mathcal{X}\}$, but increases $\Pr\{\mathcal{O}_2\}$.

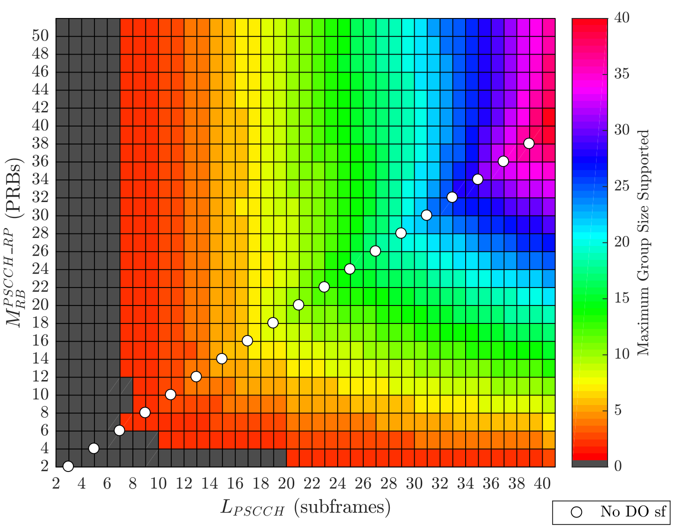

Fig. 10: Maximum D2D group size with $\Pr\{\mathcal{R}_{N_u-1}^C\} \geq 95$ % versus L_{PSCCH} and $M_{RB}^{PSCCH\_RP}$.

We also note that when $L_{PSCCH} \approx 8$ subframes, we can actually support very few UEs at the desired 95 % reliability level due to the effect of collisions. For example, when $L_{PSCCH} = 9$ subframes and $M_{RB}^{PSCCH\_RP} = 8$ PRBs, so that $N_{PSCCH} = 36$ resources, when $N_u = 4$ UEs, $\Pr\{\mathcal{X}\} = 1 - (35/36)^3 = 8.1$ %, which violates the minimum performance threshold. Were it possible for UEs to choose non-overlapping resources all the time, up to 36 UEs could be supported in this case with 100 % reliability, which is an order of magnitude increase. This suggests that basing resource index choices on the results of previous choices instead of using random selection may improve performance, which is a topic that we are investigating.

Thus, given $M_{RB}^{PSCCH\_RP}$, we can always improve the PSCCH performance by increasing L_{PSCCH}; however, a transmission period is split into the PSCCH and the PSSCH, so that increasing the size of the control pool requires reducing the duration of the PSSCH, which can decrease throughput. Therefore, the network operator must take any relevant constraints into account when designing the control pool.

V. Conclusion

In this paper, we developed an analytical model for the PSCCH in out-of-coverage scenarios where the UEs select control channel resources autonomously. We obtained the distribution of the number of UEs in a D2D group that receive a transmitted control message as a function of the PSCCH dimensions and the number of UEs in the group. This distribution can be used to generate performance metrics such as the maximum number of UEs that can be supported above a desired reliability threshold for a given resource pool configuration. Our analysis shows that the dimensioning of the resource pools has a significant and well-understood impact on the performance of the PSCCH. It is therefore possible to determine the best configuration to obtain a target performance level while minimizing the resource pool size. Finally, we note that the PSCCH is only one component of the sidelink. We are currently characterizing the performance of the PSSCH, and will use the results to examine how to optimize the transmission period to maximize sidelink throughput.

Acknowledgment

The authors would like to thank the Office for Interoperability and Compatibility of the United States Department of Homeland Security for funding this work.

References

[1] 3GPP, "Technical Specification Group Services and System Aspects; Proximity-based services (ProSe); Stage 2; TS 23.303," 3rd Generation Partnership Project (3GPP), Tech. Rep., 2016. [Online]. Available: http://www.3gpp.org/DynaReport/23303.htm

[2] 3GPP, "Technical Specification Group Radio Access Network; Study on LTE Device to Device Proximity Services; Radio Aspects; TR 36.843," 3rd Generation Partnership Project (3GPP), Tech. Rep., 2015. [Online]. Available: http://www.3gpp.org/DynaReport/36843.htm

[3] 3GPP, "Technical Specification Group Radio Access Network; Evolved Universal Terrestrial Radio Access (E-UTRA); Physical layer procedures; TS 36.213," 3rd Generation Partnership Project (3GPP), Tech. Rep., 2016. [Online]. Available: http://www.3gpp.org/DynaReport/36213.htm

[4] S. Y. Lien, C. C. Chien, F. M. Tseng, and T. C. Ho, "3GPP device-to-device communications for beyond 4G cellular networks," *IEEE Commun. Mag.*, vol. 54, no. 3, pp. 29–35, March 2016.

[5] S. Y. Lien, C. C. Chien, G. S. T. Liu, H. L. Tsai, R. Li, and Y. J. Wang, "Enhanced LTE device-to-device proximity services," *IEEE Commun. Mag.*, vol. 54, no. 12, pp. 174–182, December 2016.

[6] M. J. Shih, H. H. Liu, W. D. Shen, and H. Y. Wei, "UE autonomous resource selection for D2D communications: Explicit vs. implicit approaches," in *2016 IEEE Conf. Standards for Communications and Networking (CSCN)*, Berlin, Germany, 31 Oct–2 Nov 2016.

[7] R. A. Rouil, F. J. Cintrón, A. Ben Mosbah, and S. Gamboa Quintiliani, "A Long Term Evolution (LTE) device-to-device module for ns-3," in *Workshop on ns-3 (WNS3)*, Seattle, WA, USA, 2016.